Solid State Science and Technology, Vol. 19, No 1 (2011) 175-189
ISSN 0128-7389

PREPARATION AND CHARACTERIZATION OF NEW $Bi_{1.5-x}CuNb_{1.5+x}O_{7+x}$ PYROCHLORES

Chon Mun Ping[1,*], Tan Kar Ban[1], Khaw Chwin Chieh[2], Zulkarnain Zainal[1] and Taufiq-Yap Yun Hin[1]

[1]*Chemistry Department, Science Faculty, Universiti Putra Malaysia, 43400 UPM Serdang, Selangor*

[2]*Engineering and Science Faculty, Kuala Lumpur Campus Jalan Genting Kelang, 53300 Kuala Lumpur*

**Corresponding Author: alexischon_mp@yahoo.co.uk*

ABSTRACT

A new pyrochlore solid solution, $Bi_{1.5-x}CuNb_{1.5+x}O_{7+x}$ has been synthesized using conventional solid state method. The synthesized ceramic samples were fired at 925ºC and their phase purities were analyzed using Shimadzu XRD-6000, X-ray powder diffractometer. The refinement process was performed using Chekcell programme with Fd-3m symmetry. The cubic pyrochlore structures were confirmed with a = 10.5024 (3) Å and 10.5092 (5) Å for x = 0.1 and x = 0.2, respectively. Lattice constants of the cubic pyrochlore have been found increased with increase of Nb content. On the other hand, the resulting powder was pelletized and sintered at sintering temperature prior to impedance spectroscopy (IS) measurement. The electrical measurement was carried out in the frequency range of 0.1 Hz – 10 MHz over a temperature from room temperature to 800ºC, in both cooling and heating cycles.

Keywords: pyrochlores; impedence spectroscopy; Nb substitution;

INTRODUCTION

Electroceramics, used primarily for their electrical properties are high technological materials whose applications depend on a complex interplay of structural, processing and compositional variables [1]. The microstructure and electrical characteristics are strongly dependent on the firing condition [2] and a large number of pyrochlore materials has been synthesized with exploitable properties, such as solid oxide fuel cells (SOFCs) and a wide variety of electrical properties including ferroelectricity, piezoelectricity and semi conductivity [3], [4]-[5].

Oxide pyrochlores exhibit a wide variety of interesting physical properties especially the bismuth-based pyrochlores are found to have low sintering temperature, low dielectric losses ($\tan \delta \sim 10^{-4}$) and high dielectric constants up to 150 which make them

favorable candidates for cofired decoupling capacitors, low temperature cofired ceramics (LTCC) [6].

The general formula of the oxide pyrochlores can be written as $A_2B_2O_7$ and it is predominantly cubic and ionic in nature. The A ion is coordinated to eight oxygen atoms which can be a rare earth or an element with inert lone-pair of electrons and B ion is a six-fold coordinated element. In other words, A can be a trivalent or bivalent cation and B can be a quadrivalent or quiquevalent cation [3].

Impedance spectroscopy (IS) has played a vital role in fundamental and applied materials science in which it is a powerful technique to study the electrical properties of ceramic materials. Its usefulness in various applications makes it a favored analytical tool in materials research because IS is a relatively simple electrical measurement whose results are correlated with many variables which allows researchers to make interpretation of fundamental electrical and electronic processes easily [7].

In this work, we discuss on the dielectric properties of pyrochlore samples. The study of electrical properties in this non-stoichiometric pyrochlores has yet to be reported. The microstructure analysis has been done on single phase cubic pyrochlore and the structural study specifically types of bonding was analyzed by infrared spectroscopy.

EXPERIMENTAL PROCEDURE

All samples were prepared from high purity oxides, Bi_2O_3 (99.9%, Aldrich), CuO and Nb_2O_5 (99.995% and 99.9%, Alfa Aesar) via solid state reaction route. The samples, $Bi_{1.5-x}CuNb_{1.5+x}O_{7+x}$ ($0.1 \leq x \leq 0.4$) were weighed approximately 4 g according to their stoichiometric compositions before ground in an acetone medium using an agate mortar and pestle. The resulting powder was calcined at 900ºC for 1 day in a platinum foil and ground prior to firings at 925ºC for 2 days.

The formation of monophasic compound was confirmed by X-ray powder diffraction (XRD) analysis and the data were collected using CuKα radiation with 0.1º/min step size. The crystalline powder was pressed into pellets and sintered at 925ºC for 30 hours. The geometries of the sintered pellets were typically 7.50 (± 0.12) mm in diameters and less than 2 mm in thickness. The relative density, expressed as a percentage, is the ratio of the theoretical density to the experimental density. For $x = 0.1$ and $x = 0.2$, the relative density is ~91% and 89%, respectively.

In order to make electrical measurements, platinum electrodes were deposited on the surfaces of pellets by platinum paste. These studies were done using Solatron 1260 Impedance Spectroscopy, from room temperature up to 800ºC, on heating and cooling cycles with the incremental steps of 50ºC. The electrical properties were studied in the frequency range of 0.1 Hz to 10 MHz and the samples were analyzed based on their electrical relaxation times. Each reading was taken after thermal equilibrium for 15 minutes.

Solid State Science and Technology, Vol. 19, No 1 (2011) 175-189
ISSN 0128-7389

On the other hand, the structural and surface morphological studies have been carried out to investigate the nature of metal-oxygen bonds in these pyrochlores.

RESULTS AND DISCUSSION

In this study, a series of $Bi_{1.5-x}CuNb_{1.5+x}O_{7+x}$ solid solution has been prepared with fixed copper content, where $0.1 \leq x \leq 0.4$. The nominal composition, $x = 0$ is not found in Bi-Cu-Nb (BCN) subsolidus system. The phase purities of samples were determined by X-ray diffraction technique (CuKα radiation). Samples of $x = 0.1$ and 0.2 are confirmed phase pure cubic pyrochlores at sintering temperature of 925ºC. The compositions with $x = 0.3$ and 0.4 are found to be mixed phase with excess of $CuNb_2O_6$ and $BiNbO_4$. The X-ray diffraction patterns as shown in figure 1 are fully indexed in a faced-centred pyrochlore-type cubic structure and compositions with extra phases are denoted in other symbols which are shown in figure 2. The Miller indices of $Bi_{1.3}CuNb_{1.7}O_{7.2}$ and $Bi_{1.4}CuNb_{1.6}O_{7.1}$ are obtained from the Chekcell refinement program. Table 1 displays the indexed values of $x = 0.2$ and the samples have negligible weight loss during the annealing process.

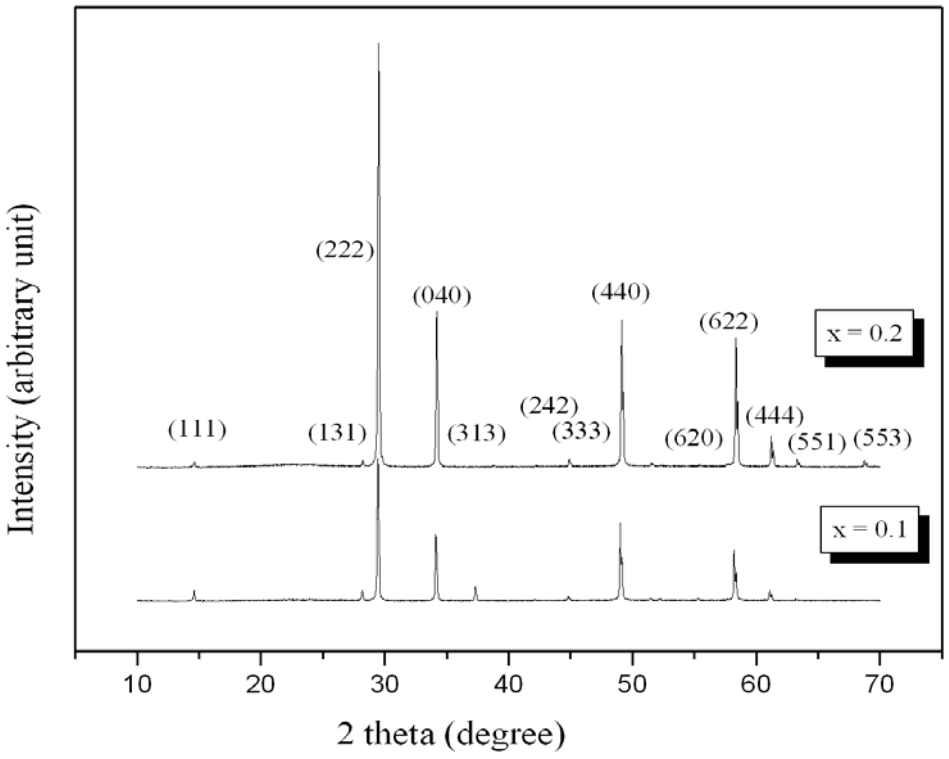

Figure 1: XRD patterns of single phase compositions, $x = 0.1$, 0.2

Solid State Science and Technology, Vol. 19, No 1 (2011) 175-189
ISSN 0128-7389

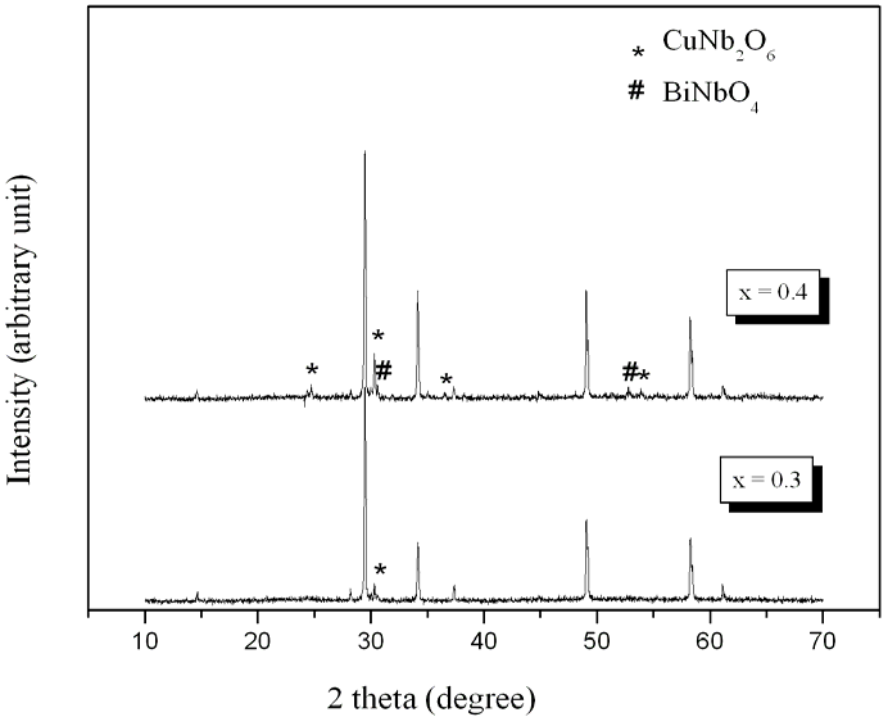

Figure 2: X-ray diffraction patterns of mixed phase ceramic materials

Table 1: Miller indices, *hkl* of x = 0.2

2θ (Obs)	2θ (Cal)	Intensity (counts)	H	K	L
14.564	14.592	415	1	1	1
28.128	28.147	278	1	3	1
29.407	29.427	11509	2	2	2
34.095	34.108	3070	0	4	0
37.273	37.276	882	3	1	3
42.076	42.100	61	2	4	2
44.798	44.788	375	3	3	3
49.013	49.007	5289	4	4	0
55.24	55.253	70	6	2	0
58.214	58.201	3796	6	2	2
61.053	61.057	1162	4	4	4
63.155	63.148	65	5	5	1
68.56	68.551	59	5	5	3

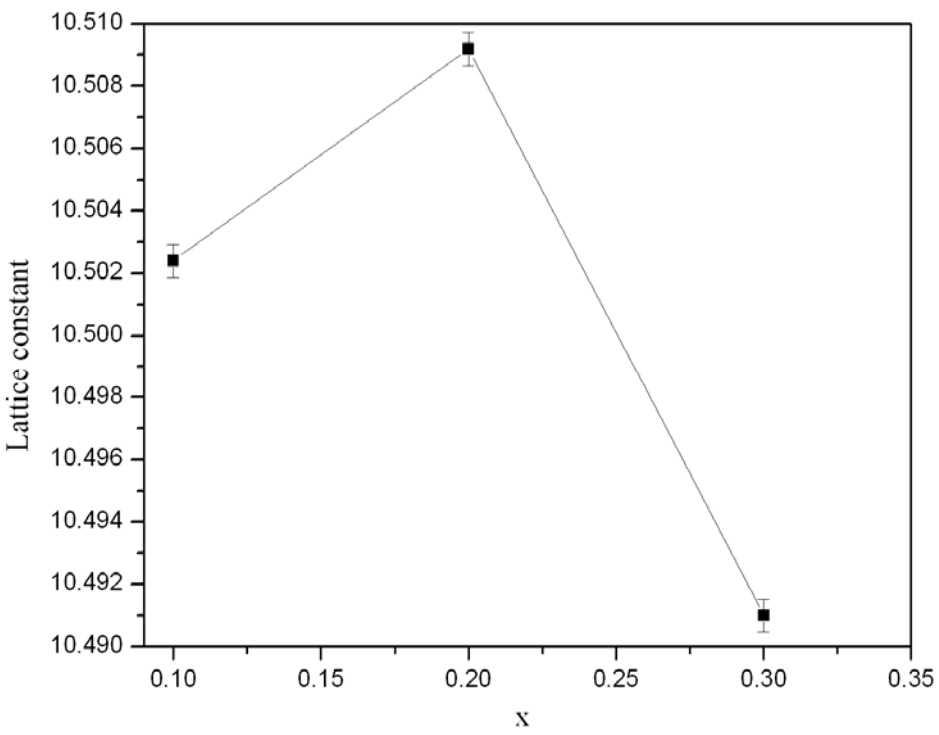

Figure 3: Lattice constant as a function of x in $Bi_{1.5-x}CuNb_{1.5+x}O_{7+x}$ series

Figure 3 shows the variation of lattice constant as a function of niobium content. From the observation, the lattice constant increases with higher x values where x = 0.1 and 0.2 but decreases when x = 0.3. The discontinuity of x = 0.3 indicates the emergence of secondary phase in which the solid solution limit is achieved.

Electrical properties

Table 2 shows the values of dielectric permittivity (ε') and loss tangent (tan δ) of BCN system at different frequencies. The variations of ε' and tan δ as a function of temperature and frequency are plotted in figures 4 - 8.

Generally, $Bi_{1.4}CuNb_{1.6}O_{7.1}$ has higher ε' and tan δ with respect to $Bi_{1.3}CuNb_{1.7}O_{7.2}$ at the corresponding frequency. Both samples exhibit high losses and it is speculated that Cu ion changes its valence state at elevated temperature [6]. Higher temperature will stimulate the thermal activation process and hence the conduction mechanism is facilitated [8]. On the other hand, the dielectric losses are much lower at high frequency than the one occurring at low frequency (figure 5) and this frequency dependent behavior is typically observed in pyrochlore materials [9].

Table 2: Values of ε' and tan δ of BCN for a) room temperature and b) 400ºC at 10^5 Hz and 10^6 Hz, respectively

	$Bi_{1.4}CuNb_{1.6}O_{7.1}$		$Bi_{1.3}CuNb_{1.7}O_{7.2}$	
a)	ε'	tan δ	ε'	tan δ
100 kHz	49.05	0.71	40.51	0.52
1 MHz	39.24	0.33	36.29	0.25
b)	ε'	tan δ	ε'	tan δ
100 kHz	814.01	2.88	507.98	2.87
1 MHz	280.26	1.57	189.78	1.47

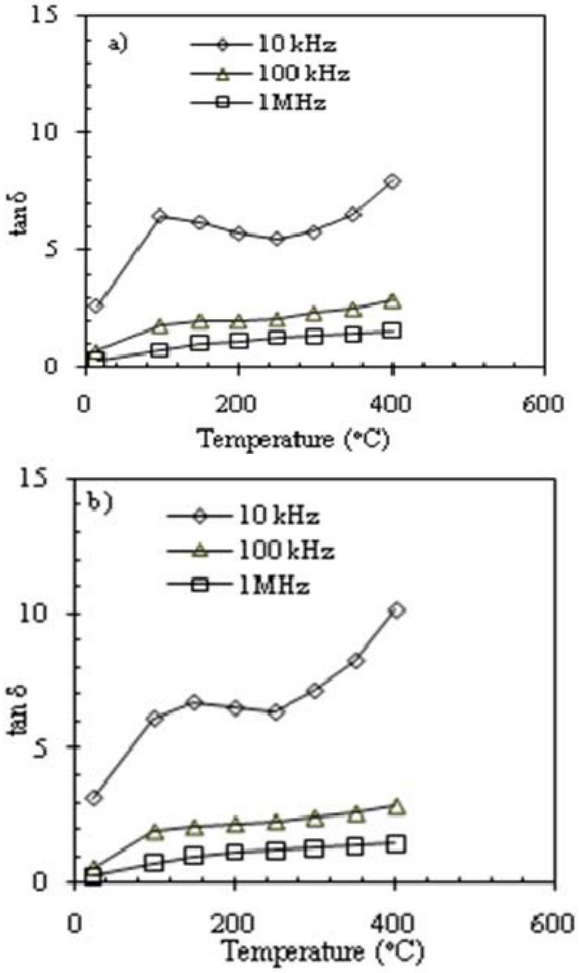

Figure 4: tan δ as a function of temperature at 10 kHz, 100 kHz and 1 MHz for a) $Bi_{1.4}CuNb_{1.6}O_{7.1}$ b) $Bi_{1.3}CuNb_{1.7}O_{7.2}$

There is a high degree of dispersion of ε' below 10 kHz (figure 6) and the values increase rapidly at lower frequency but decrease linearly at higher frequency (figure 7). In other words, ε' increases significantly with temperature at low frequency and this behavior is commonly observed in ferroelectric materials. There are five possible types of polarizations occur in the material namely interfacial, dipolar, atomic, ionic and electronic conduction which giving rise to higher values of ε' at low frequencies [10].

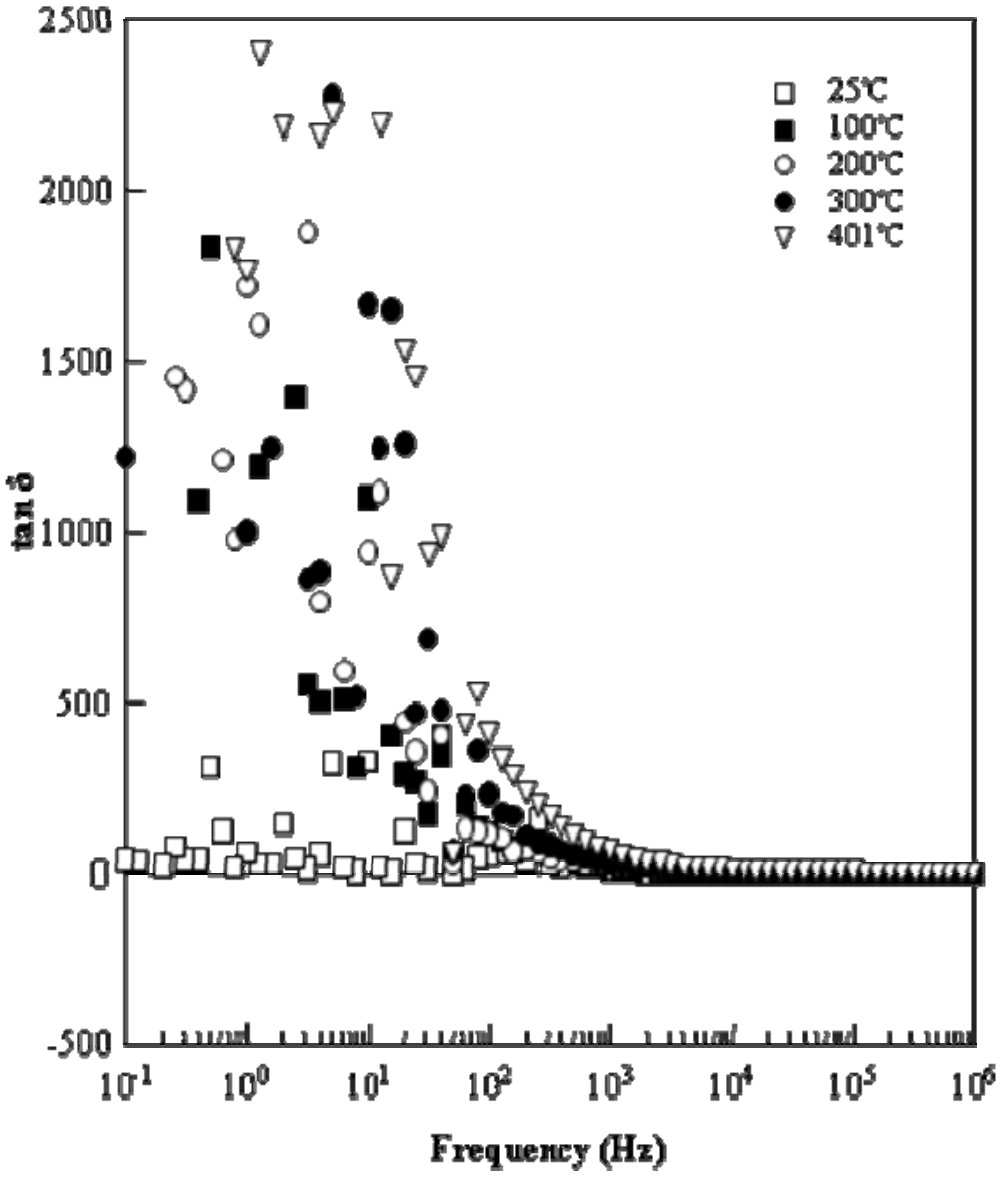

Figure 5: Dieletric loss as a function of frequency for $Bi_{1.3}CuNb_{1.7}O_{7.2}$ at different temperatures

Solid State Science and Technology, Vol. 19, No 1 (2011) 175-189
ISSN 0128-7389

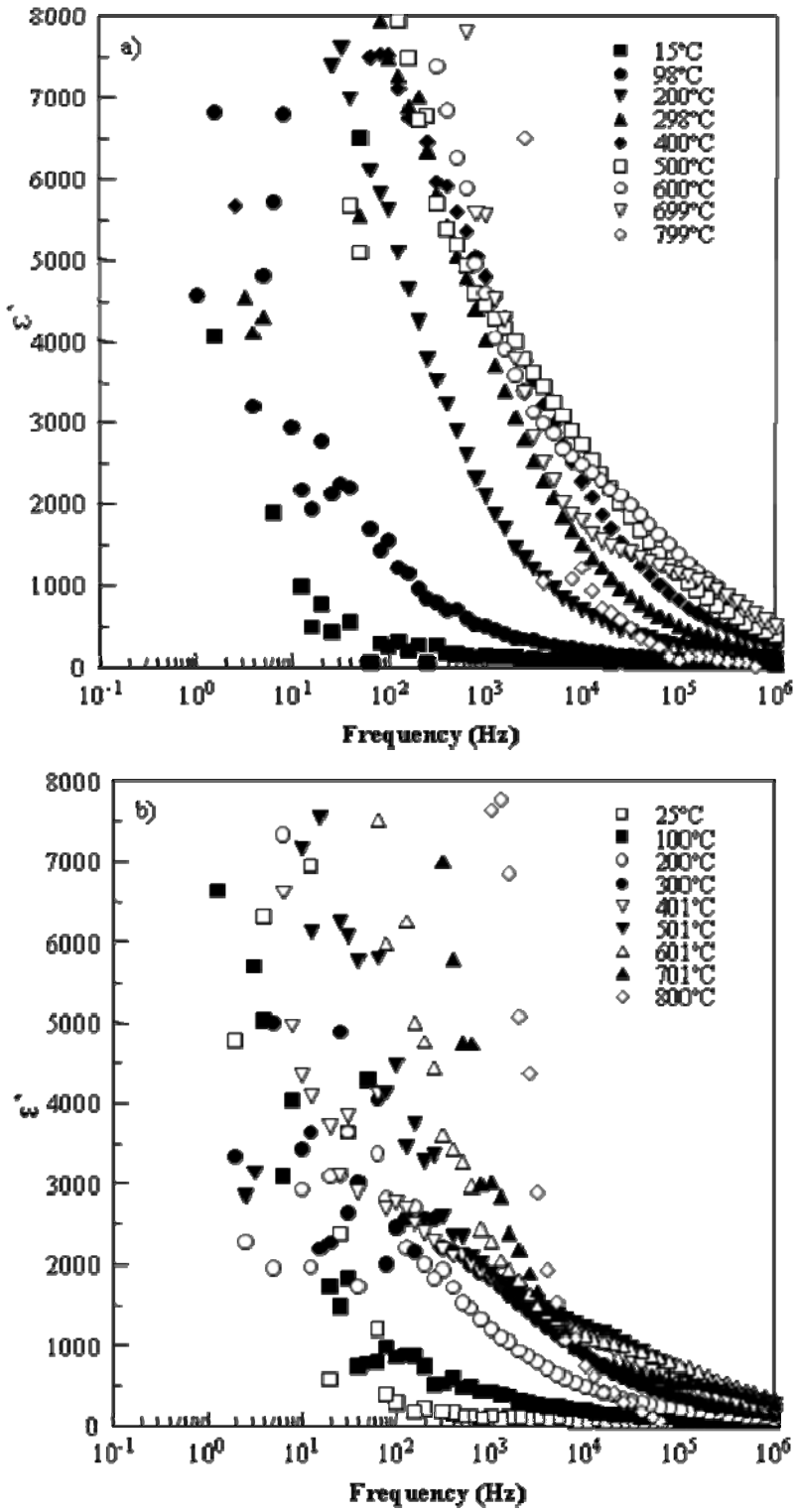

Figure 6: Real part of the dielectric permittivity measured as a function of frequency where a) $Bi_{1.4}CuNb_{1.6}O_{7.1}$ b) $Bi_{1.3}CuNb_{1.7}O_{7.2}$

In general, ε' and tan δ are temperature dependent. In this study, ε' values are considerable high in both pyrochlores and this observation is due to the occurrence of dielectric polarization in the materials in which the electrical conductivity increases with temperature where the hopping conduction mechanism is likely taken place [11].

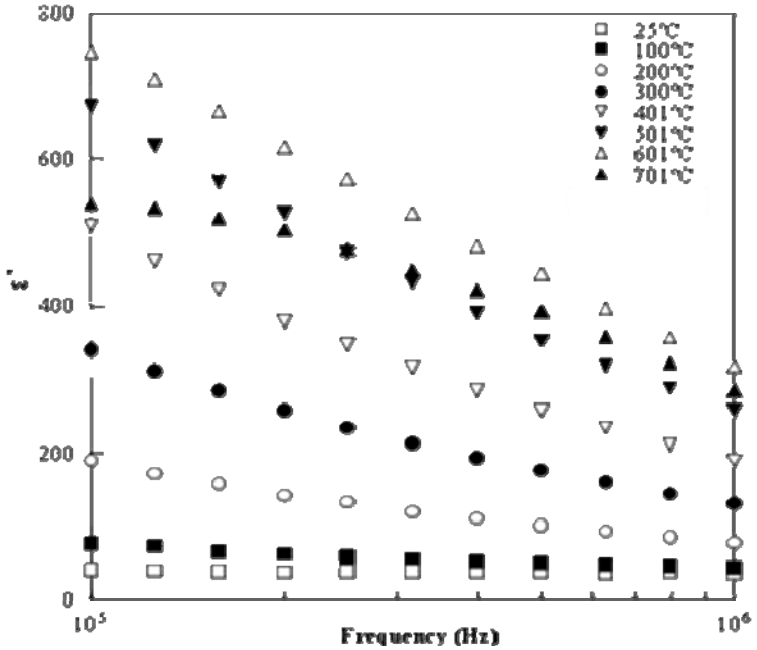

Figure 7: Dielectric permittivity response of $Bi_{1.3}CuNb_{1.7}O_{7.2}$ at high frequency region

Figure 9 delineates the imaginary part of Z'' as a function of frequency. The maximum of the curve implies the existence of polarization in the samples [12] and the peaks decrease with increase of temperature where the maxima are slightly displaced towards higher frequency region.

The collected impedance data are modeled in complex Cole-cole plots, e. g. Z'' vs Z'. The perfect semicircle could be represented with a set of parallel RC elements [13] as shown in inset figure 10 and the BCN system exhibits semicircle at temperature less than 100ºC. The capacitance values of $Bi_{1.4}CuNb_{1.6}O_{7.1}$ and $Bi_{1.3}CuNb_{1.7}O_{7.2}$ are within the order of 10^{-12}, where this region is dominated by bulk boundary component [1].
Figure 11 displays the Arrhenius conductivity plots of $Bi_{1.4}CuNb_{1.6}O_{7.1}$ and $Bi_{1.3}CuNb_{1.7}O_{7.2}$ measured at 1 MHz. The activation energies of x = 0.1 and x = 0.2 are 0.154 eV and 0.156 eV, respectively.

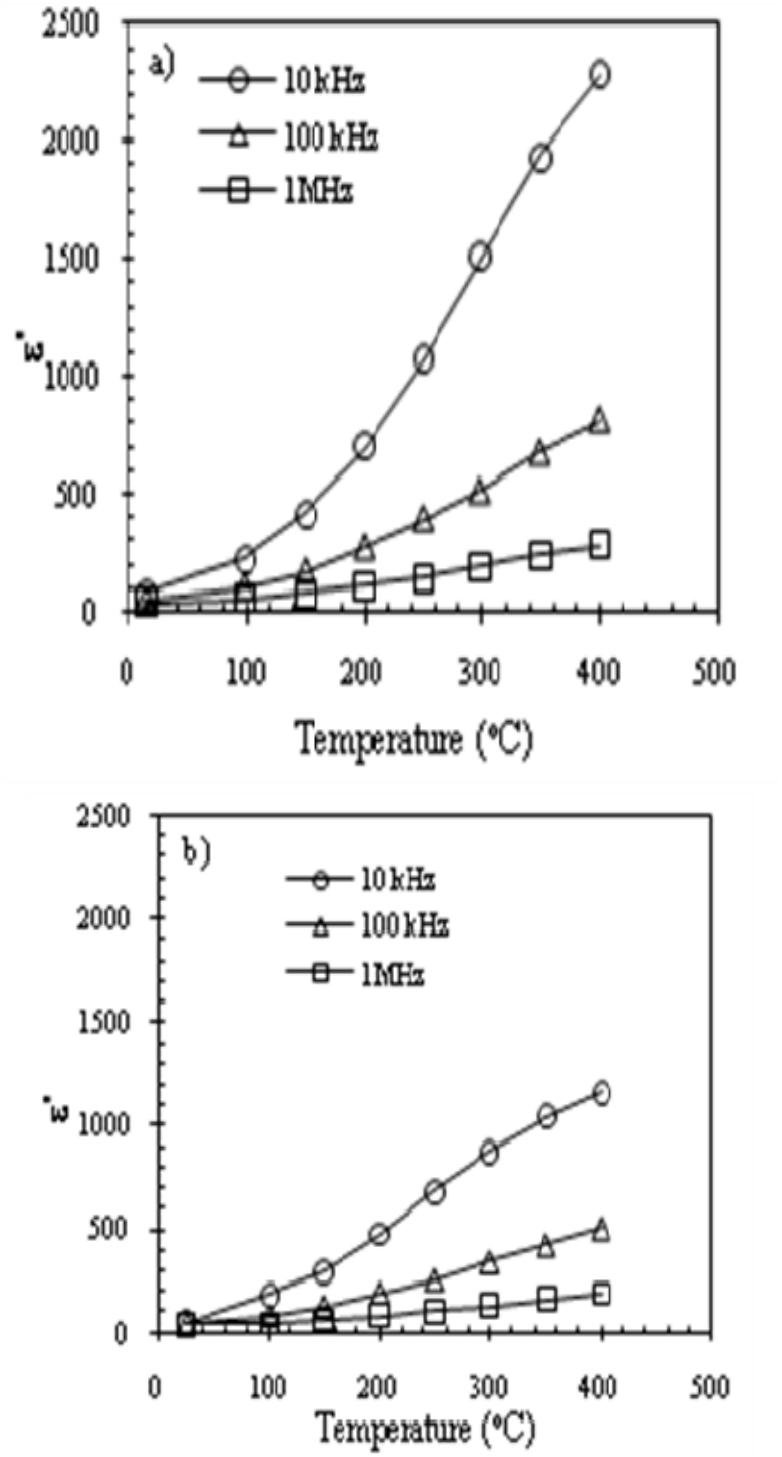

Figure 8: ε' as a function of temperature at 10 KHz, 100 KHz and 1 MHz of a) $Bi_{1.4}CuNb_{1.6}O_{7.1}$ b) $Bi_{1.3}CuNb_{1.7}O_{7.2}$

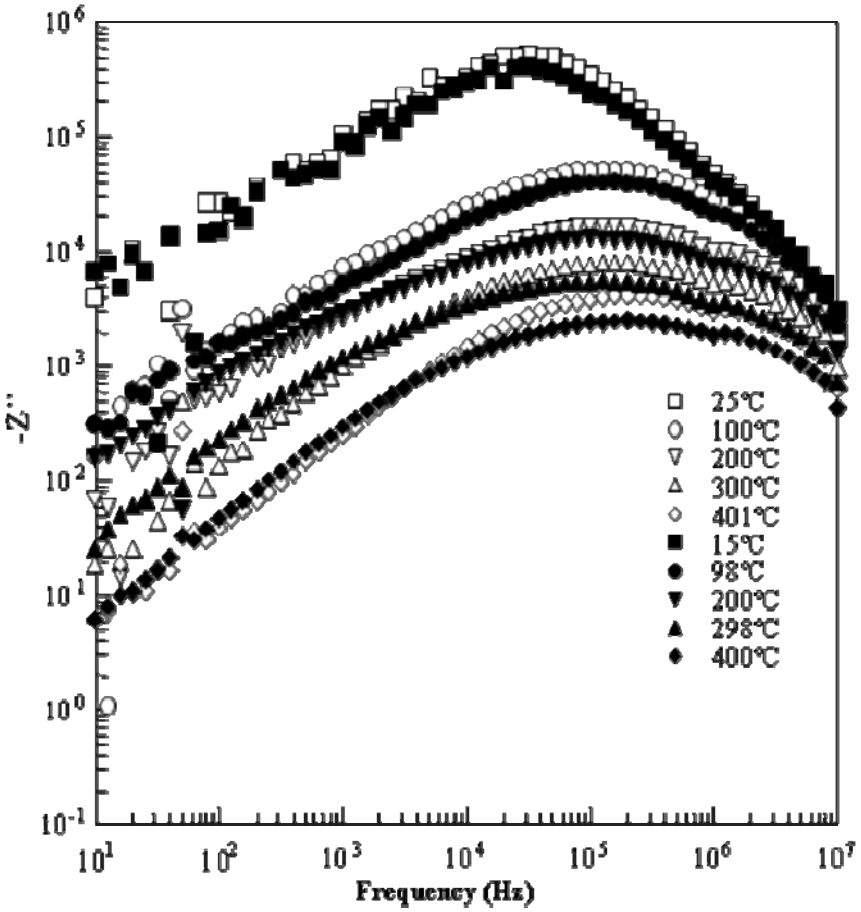

Figure 9: Combination of imaginary part of Z* as a function of frequency, a) open shape: $Bi_{1.4}CuNb_{1.6}O_{7.1}$ b) filled shape: $Bi_{1.3}CuNb_{1.7}O_{7.2}$

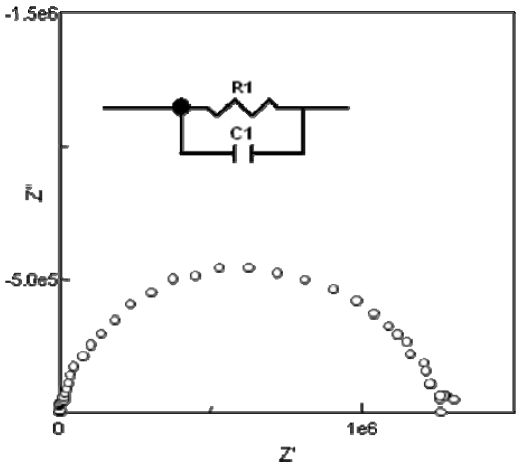

Figure 10: Cole-cole plot of $Bi_{1.3}CuNb_{1.7}O_{7.2}$ at room temperature, 25ºC

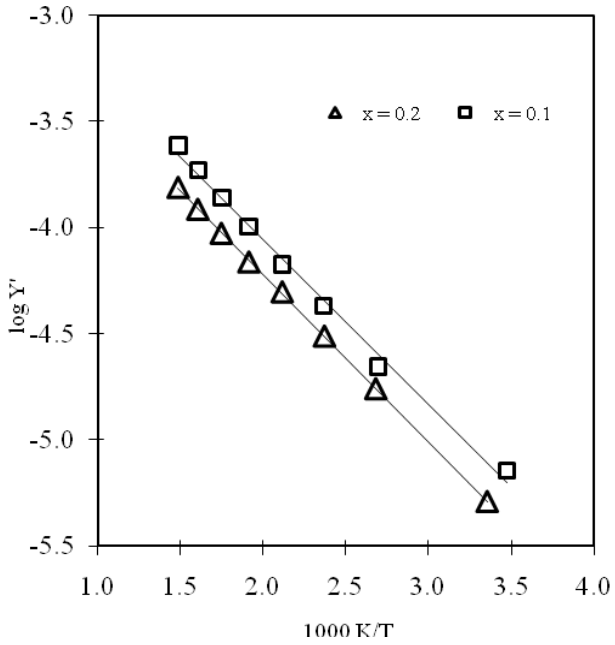

Figure 11: Arrhenius conductivity plots of BCN pyrochlores

Structural and compositional analyses

Fourier transform infrared spectroscopy (FTIR) was used to characterize Bi-based ceramic materials. The spectra of $Bi_{1.4}CuNb_{1.6}O_{7.1}$ and $Bi_{1.3}CuNb_{1.7}O_{7.2}$ were recorded in 4000.0 – 280.0 cm^{-1} range. The absorption peak located at approximately 860.0 cm^{-1} is attributed to the B-O-B stretching mode, in which the Nb-O-Nb applied in this case. The most intense absorption peaks observed in both $Bi_{1.4}CuNb_{1.6}O_{7.1}$ and $Bi_{1.3}CuNb_{1.7}O_{7.2}$ samples are featured to be Nb-O stretching mode, at ~534.0 – 564.0 cm^{-1} [14]. On the other hand, the peaks situated at ~330.0 cm^{-1} are corresponded to AO stretching vibration frequency (ν). There are two possible types of bonding coincide at this ν, namely Bi-O and Cu-O absorption bands. Therefore, a careful assessment is required in order to understand the nature of pyrochlores. Considering the atomic weight of Bi is much greater than Cu, it is rationale to assign the stretching ν to be Bi-O rather than Cu-O due to the reason of the lower ν, the heavier the mass of the atoms [15]. Also, $Bi_{1.4}CuNb_{1.6}O_{7.1}$ exhibits a less intense peak than that of $Bi_{1.3}CuNb_{1.7}O_{7.2}$ at 327.78 cm^{-1}.

Surface morphologies of the prepared samples were examined using scanning electron microscopy, LEO 1455 VPSEM and the photographs are shown in figure 13. The scanning was performed on the densified pellets with goal paste sputtered on the surface. From the SEM micrographs, x = 0.1 is more porous as compared to that of x = 0.2 and the grain size of the samples are slightly larger for lower Bi content. In addition, x = 0.2 has a little increment in the lattice constant in which the niobium content is reduced to x = 0.1. Hence, the growth of grain size is somewhat related to the lattice constant [16].

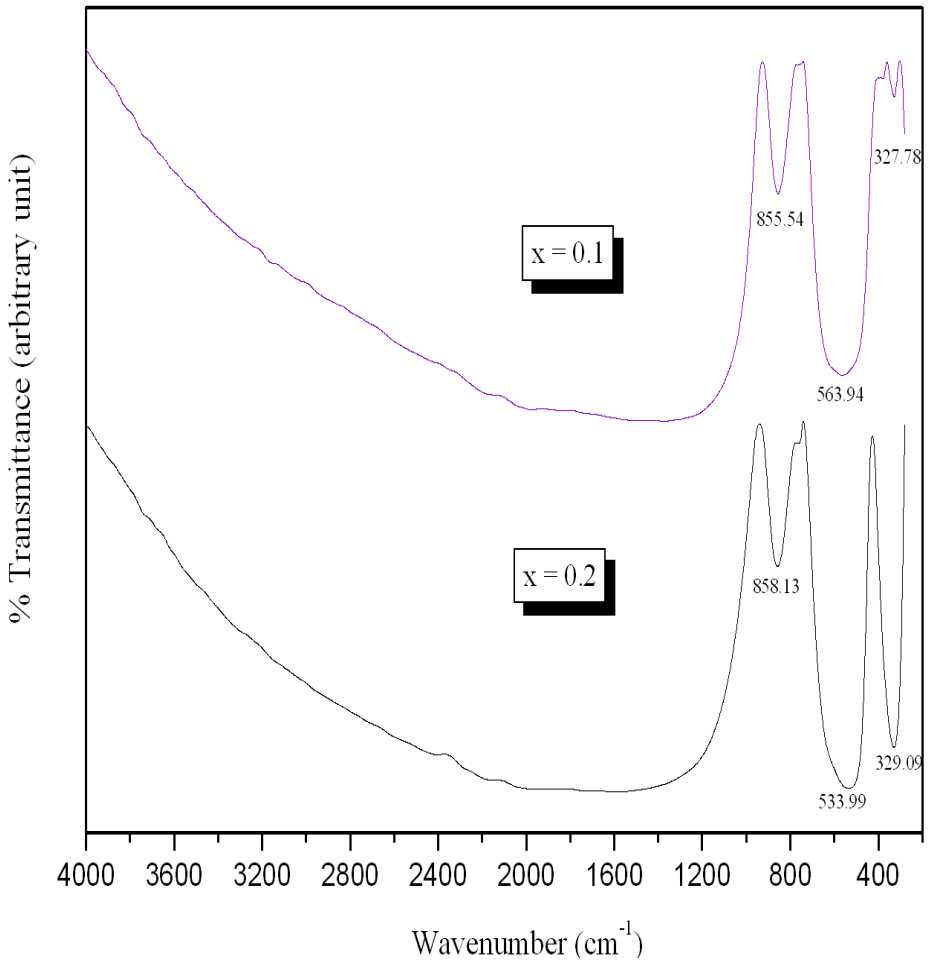

Figure 12: IR spectra of BCN

The annealing condition could contribute to the effect of the growth rate of crystal size in which it is corresponded to the different diffusion rate of the ionic species. Oxygen concentration is also believed to be the controlling factor for grain growth rate in the diffusion mechanism [17].

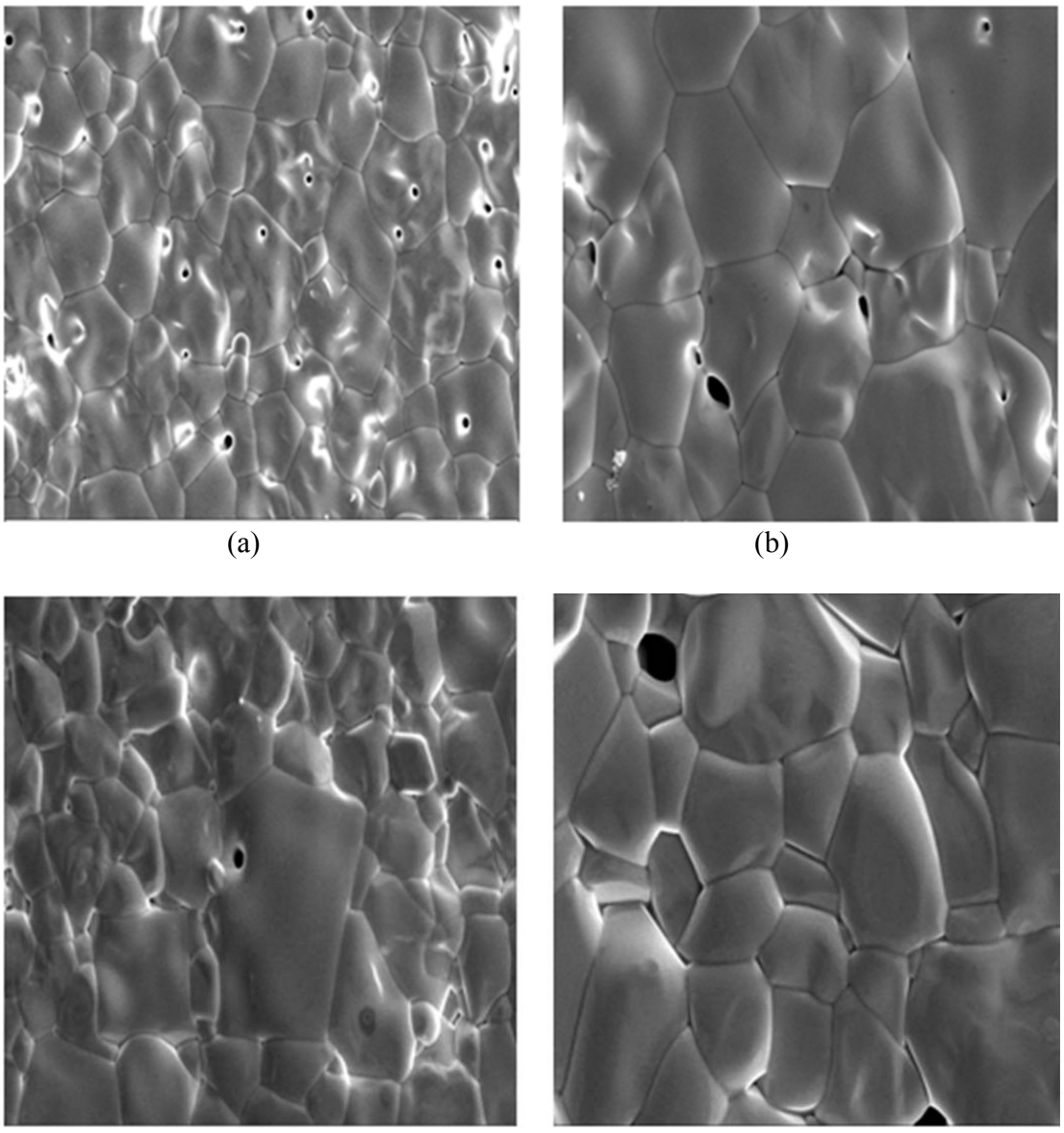

(a) (b)

(c) (d)

Figure 13: SEM micrographs taken at different magnifications. (a) and (b): 500 x and 1000 x for $Bi_{1.4}CuNb_{1.6}O_{7.1}$. (c) and (d): 500 x and 1000 x for $Bi_{1.3}CuNb_{1.7}O_{7.2}$

CONCLUSIONS

Two non-stoichiometric pyrochlores were prepared and characterized. A high dispersion of ε' and tan δ are observed in these materials in low frequency region. The values of dielectric permittivity and dielectric loss increased substantially with temperature in which the hopping conduction mechanism is probable taken place. The possible polarization in the sample could be due to electronic conduction which corresponds to the great dielectric losses in the samples. Nearly perfect semicircles are

discernable at much lower temperature which indicates the electrical response is likely attributed to the bulk behavior.

ACKNOWLEDGMENTS

We thank Ministry of Higher Education through the Fundamental Research Grant (FRGS 02-11-08-620FR) and M. P. Chon is grateful for her National Science Fellowship (NSF) from Ministry of Science, Technology, and Innovation Malaysia (MOSTI).

REFERENCES

[1] J. T. S. Irvine, D. C. Sinclair and A. R. West. *Advanced Materials,* **2** (3) (1990) 132
[2] B. S. Prakash and K. B. R. Varma. *Journal of Materials Science*, **42** (2007) 7467-7477
[3] M. A. Subramanian, G. Aravamudan and G. V. Subba Rao. **15** (1983) 55-143
[4] V.V. Kharton, F. M. B. Marques and A. Atkinson. *Solid State Ionics*, **174** (2004) 135-149
[5] C.A. Randall, J.C. Nino, A. Baker, H-J. Youn, A. Hitomi, R. Thayer, L.E. Edge, T. Sogabe, D. Anderson, T.R. Shrout, S. Trolier-Mckinstry, and M.T Lanagan, *American Ceramic Society Bulletin,* (2003) 9101-9108
[6] D. P. Cann, C. A. Randall and T. R. Shrout. *Solid State Communications*, **100** (7) (1996) 529-534
[7] E. Barsoukov and J. R. Macdonald. "Impedance spectroscopy theory, experiment, and applications", 2nd ed., (A John Wiley & Sons, Inc., New Jersey, 2005), 9
[8] P. Q. Mantas. *Journal of the European Ceramic Society*, **19** (1999) 2079-2086.
[9] H. Du and X. Yao. *Materials Science and Engineering*, B00 (2003) 1-4.
[10] U. Intatha, S. Eitssayeam, J. Wang and T. Tunkasiri. *Current Applied Physics*, **10** (1) (2010) 21-25
[11] A. R. Shitre, V. B. Kawade, G. K. Bichile and K. M. Jadhav. *Materials Letters*, **56** (2002) 188-193
[12] M. A. L. Nobre and S. Lanfredi. *Journal of Materials Science*: *Materials in Electronics*, **13** (2002) 235-238
[13] D. C. Sinclair, F. D. Morrison and A. R. West. *International Ceramics*, Issue 2, (2000) 33-36
[14] J.-P. Masse, H. Szymanowski, O. Zabeida, A. Amassian, J.E. Klemberg-Sapieha and L. Martinu *Thin Solid Films*, **515** (2006) 1674-1682
[15] P. P. Rao, S. J. Liji, K. R. Nair and P. Koshy. *Materials Letters*, **58** (2004) 1924-1927
[16] Y. Hu and C. L. Huang. *Ceramics International*, **30** (2004) 2241-2246
[17] P. J. Wilde and C. R. A. Catlow. *Solid State Ionics*, **112** (1998) 173-183